IEEE Access
Multidisciplinary | Rapid Review | Open Access Journal

Received October 4, 2021, accepted October 18, 2021, date of publication October 28, 2021, date of current version November 8, 2021.

Digital Object Identifier 10.1109/ACCESS.2021.3124098

Breakdown Voltage of Transformer Oil Containing Cellulose Particle Contamination With and Without Bridge Formation Under Lightning Impulse Stress

SARIZAN BIN SAAIDON[1,2], MOHD AIZAM TALIB[3], MOHAMAD NUR KHAIRUL HAFIZI ROHANI[4], NOR ASIAH MUHAMAD[1,5], (Member, IEEE), AND MOHAMAD KAMAROL MOHD JAMIL[1], (Senior Member, IEEE)

[1]School of Electrical and Electronic Engineering, Engineering Campus, Universiti Sains Malaysia, Nibong Tebal, Pulau Pinang 14300, Malaysia
[2]Centre for Instructor and Advanced Skill Training, Shah Alam, Selangor 40300, Malaysia
[3]TNB Research Sdn. Bhd. Research Institution Area, Kajang, Selangor 43000, Malaysia
[4]Faculty of Electrical Engineering Technology, Universiti Malaysia Perlis, Perlis 02600, Malaysia
[5]Faculty of Engineering, Universiti Teknologi Brunei, Gadong BE1410, Brunei

Corresponding author: Mohamad Kamarol Mohd Jamil (eekamarol@usm.my)

This work was supported in part by the Ministry of Education Malaysia under Grant FRGS/1/2020/TK0/USM/02/26 (Project ID: 18120), and in part by Universiti Sains Malaysia.

ABSTRACT This study investigates the effect of cellulose bridge formation on insulating oil. Such effect influences the breakdown voltage and strength of mineral oil (MO) under standard lightning impulse (LI) voltage. A cylindrical test vessel fitted with spherical–spherical electrodes with a 2 mm gap distance between them was used to generate a quasi-uniform field and observe bridge formation between the gaps. A positive LI waveform (1.2/50 μs) generated by an impulse generator was applied during the breakdown tests. The rising-voltage method was used to measure the breakdown voltage in accordance with the IEC 60897 standard test method. Weibull cumulative breakdown probability was applied to present the breakdown results statistically, and the outcome was compared with clean oil (CO). Commercial cellulose microcrystalline particles were dispersed into the transformer oil to act as bridge. The concentrations of the samples were 0.004%, 0.008% and 0.012% by weight. The breakdown test results showed that the cellulosic particles reduced the LI breakdown voltage (LIBV) of MO by up to 10%. The influence of cellulose particles on LIBV was also more prominent during bridge formation, with a further reduction of 14%. Evidently, the presence of the cellulose bridge exerted a detrimental effect on the breakdown voltage of MO under LI stress, yielding a reduction of 24% and 27% at 0.004 wt% and 0.012 wt%, respectively. Finite element analysis also indicated that the electrical field strength of cellulosic particle contamination of 0.004 wt% and 0.012 wt% without a bridge skeleton exceeded the critical electric field strength of CO by 20% and 61%, respectively. The presence of cellulosic contamination at any concentration, i.e. either with or without a bridge structure, clearly decreased the breakdown strength of transformer oil. However, the breakdown is not occurred instantaneously. The LI breakdown was initiated and established only at a certain impulse stress level, when the electric field strength along the bridge lines exceeded the critical electric field strength of the oil. Thus, this finding potentially contributes to the formulation of guidelines for condition assessment and contamination monitoring to minimise common issues in power transformer failures that are attributable to the insulation system, and consequently, achieve optimum transformer insulation integrity.

INDEX TERMS Quasi-uniform field, cellulose particle bridging, breakdown voltage, lightning impulse stress.

I. INTRODUCTION

Mineral oil (MO) and pressboard are traditionally selected as dielectric systems to elicit the best insulating and heat evacuation for a reliable long-time operation on the basis of condition diagnosis and assessment [1], [2]. However, both materials are inevitably exposed to stresses during normal operations because of thermal, mechanical, electrical and chemical reactions [3]. These stresses and reactions degrade the pressboard by breaking the polymer chains that are linked

The associate editor coordinating the review of this manuscript and approving it for publication was Guillaume Parent.

to form dust particles, reducing its degree of polymerisation [4] and then producing dust particles dispersed into oil as by-product contamination. These cellulose particles tend to gravitate towards the high-field region because of the dielectrophoresis effect [5], which leads to the formation of a cellulose bridge when particles are polarised [6]. Under the control of particle interaction forces, movement occurs at the strongest region of field stress [6]–[8]. If the present cellulose particles are large, then forces tend to accelerate these particles to align in parallel within electric field lines, potentially customising a bridge across the gap over a certain period [9]. The bridge probably increases local field enhancement and operates as a conducting path by authorising conductivity activity amongst different transformer structures. This conducting path cause the insulating properties to become severe and can lead to pre-breakdown and breakdown in the transformer, increasing the possibilities of insulation failure [10]–[15]. If cellulose concentration is insufficient for bridging the gaps, then cellulose particles tend to increase local field enhancement, and breakdown events will occur locally amongst close-knit cellulose particles [9].

The lightning impulse (LI) breakdown test plays an important role in the insulation system of transformers. As a basic criterion for designing an insulation system, insulation strength has to fulfill a basic insulation level (BIL) that is required by transformer manufacturers [16] to ensure that transformer performance can withstand lightning overvoltage. In accordance with the International Electrotechnical Commission (IEC) 60076-3 standard, lightning and switching impulse tests are compulsory for all transformers operated at a rated voltage exceeding 72.5 kV [17]. However, the performance of a transformer completely depends on the performance of an insulation system in terms of withstanding disturbances during operation even when its passes the test. Sokolov and Lokhanin [18] identified common issues in power transformer failures as insulation, tap-changer and bushing failures. Failures attributed to the insulation system or insulating oil contamination due to particles are reported as major factors that contribute more than 30% of total transformer breakdown [18], [19]. Over time, insulation age degrades the performance of transformers because contamination occurs due to several stresses in dielectric liquids, particularly in high-voltage power transformers [13]. Cellulose particles are identified as contaminants in dielectric liquids. Miyao *et al.* [20] found that 95% of contaminations in transformer oil originate from cellulose particles.

The underlying breakdown mechanism of an insulation system due to cellulose contamination, which leads to transformer breakdown, is intrinsically complex; studies are currently being conducted to understand this mechanism [21], [22]. The initiation and propagation of a breakdown and the effect of contamination on this process remain unclear. At present, no single theory that focuses on contamination can summarise all the processes that lead to breakdown in dielectric liquid.

Most previous investigations focused on conductivity caused by oil contamination. Other researchers investigated the influence of LI on streamer characteristics (with and without pressboard interface) or the breakdown and withstand voltage of various insulating oils in a field [23]. One study examined the effects of electrodes, impulse shape, nature of dielectric liquid and cellulose particles [24].

Another study [25] demonstrated that cellulose concentration affects the impulse breakdown of dielectric liquid. This study focused on the breakdown mechanism of synthetic and natural ester liquids under the influence of standard LI voltage wherein MO measurements were used as benchmark. The results showed that the breakdown voltage of ester and MO was significantly reduced by 50% in the presence of cellulose particles. The breakdown voltage was reduced further in the presence of moisture and cellulose particles. This finding established that effective stressed area, duration of electric stress and liquid viscosity are factors that distress breakdown strength in dielectric liquid. However, studies have focused on investigating the effects of impulse voltage on the dielectric strength of fresh and contaminated oil samples without considering the occurrence of bridge formation.

To date, no research has yet examined stress caused by LI on breakdown strength due to contamination at different concentrations with bridge formation. Therefore, the objectives of this paper are to investigate and evaluate the breakdown voltage of MO contaminated with cellulose particles in a quasi-uniform field with and without a bridge subjected to LI stress. The breakdown voltage of fresh MO was always used as the baseline reference. The results of the experiments showed that cellulose contamination clearly curtail the breakdown voltage of transformer oil. The influence of cellulose particles was also more pronounced on bridge formation, with further reduction in breakdown strength. The findings established that the presence of cellulose contaminants in MO is evident from the decrease in the breakdown voltage of MO and more prominent when cellulose particles are in form of a cellulose bridge. Although cellulose bridges the gap, the breakdown is not instantaneously occurred. The electric field distribution and intensity play crucial roles in determining breakdown occurrence when they exceed the critical field of CO.

II. EXPERIMENTAL SETUP

A. SAMPLE PREPARATION

Nytro Gemini X (naphthenic) high-grade MO was used for the test samples in this study [26]. Firstly, to exclude moisture that may interfere with the test results, a bulk quantity of MO was collected from a sealed barrel, and the oil was pretreated by degassing in a vacuum oven set at 75 °C for more than 48 h. Secondly, the oil was allowed to cool to room temperature (30 °C $\pm$ 3 °C) [27] for 24 h under vacuum. The moisture content of MO was determined using the Karl Fischer titration method. The pretreated oil sample was denoted as

clean oil (CO). The moisture content of CO was 6.08 ppm. Once the cylindrical test cell was slowly filled with MO, the oil was allowed to settle for 5 min prior to conducting the experiments to prevent the formation of gas bubbles.

Microcrystalline cellulose powder [28] with a particle size of 20 μm was dehydrated in a vacuum oven set at 75 °C for 8 h to remove moisture, which may be absorbed during the preparation of the samples. The cellulose powder was allowed to cool to room temperature (30 °C + 3 °C) for 6 h under vacuum condition. Subsequently, a magnetic stirrer was used to disperse the cellulose particles uniformly in MO to prevent the formation of cloud-like or cotton-like clusters of cellulose particles. Finally, the test samples were placed in a vacuum drying oven wherein pressure was set to 100 Pa and temperature was maintained at 75 °C. The test samples were labelled as the non-bridging contaminated processed oil sample (NB_CPS) and the bridging contaminated processed oil sample (B_CPS). The concentrations of cellulose particles as established in [6], [14] were detailed as follows: 0.004 wt%, 0.008 wt% and 0.012 wt%. The moisture content of all the processed samples was 6–8 ppm.

B. ELECTRODE CONFIGURATION SYSTEM

A cylindrical test cell with a capacity of 300 ml and with a spherical–spherical electrode configuration was utilised in the experiment to replicate the real quasi-uniform field in an actual transformer. The cylindrical test cell was made of transparent Perspex sheet to enhance observation of bridging images. The spherical electrodes were made of AISI 52100 chromium steel. Each electrode had a diameter of 13 mm, and the gap distance was fixed at 2 mm. The 2 mm gap was the most appropriate distance for creating and retaining an artificial bridge skeleton under a direct current (DC) field as established in [6], [29], and [30]. Prior to the experiments, all parts of the electrode configuration system were washed with detergent and rinsed thoroughly with hot water. Lastly, the parts were rinsed with distilled water. A forced convection laboratory oven that was set at 80 °C for 20 min was used to dry the parts and eliminate any remaining moisture.

C. IMPULSE GENERATOR AND TESTING METHOD

Figure 1 shows the schematic of the experimental setup. A 140kV impulse generator with an energy of 250 J was used to provide a standard positive LI voltage waveform of 1.2/50 μs. The DC output voltage waveform was measured using a high-voltage capacitive divider. For the bridging experiment, +10 kV DC power supply was controlled to accelerate bridge formation within the electrode gap. The bridge formed as early as 30 s and was controlled by the strong electric field. Subsequently, DC power supply decreased to +2 kV to retain the bridge structure before shooting the impulse voltage. Tests were conducted at room temperature (30 °C $\pm$ 3 °C), as suggested by the procedure outlined in IEC 60897 [27]. Positive LI and negative LI are necessary for the insulation test. However, the current study focused on the positive waveform. Thus, a positive LI voltage

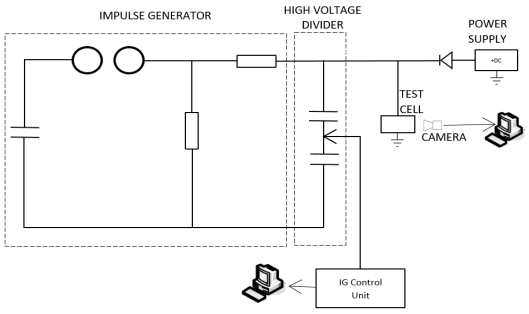

FIGURE 1. Diagram of the experimental electrical setup.

with a standard waveform of 1.2 (±30%)/50 (±20%) μs was supplied to the spherical electrode gap.

The rising-voltage method was used in the current study. The step voltage was increased by 5 kV (ΔU) at every shot until breakdown occurred in MO. The time interval (ΔT_1) between two consecutive successive impulses was 60 s to allow the test sample to settle before another impulse was shot. These procedures were repeated until 20 breakdowns occurred in the liquid. Figure 2 illustrates the concept of the rising-voltage method, where ΔT_1 denotes the time interval between two consecutive impulse shots, ΔT_2 denotes the time interval between two consecutive tests and ΔU is the step voltage increment.

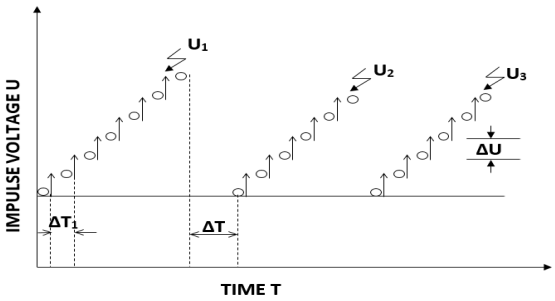

FIGURE 2. Rising-voltage method.

A total of 20 breakdowns were realised for each test sample, i.e. CO, NB_CPS and B_CPS at different concentrations. To statistically analyse the effects of cellulose and its bridge skeleton on the breakdown voltage of MO, the Weibull cumulative breakdown probability plot [31] was used to estimate breakdown voltage at 50% probability. This probability can be used as an indicator of effective impulse shot to prove the occurrence of breakdown [32], [33] in a liquid.

Weibull distribution was optimised to analyse breakdown data distribution or the law of insulation failure [34]. The Weibull distribution function is given in Equation (1), wherein 50% of the breakdown probabilities were determined for the CO and contaminated oil samples with and without bridge formation.

$$F_{Weibull}(x) = 1 - e^{-\left(\frac{x}{\beta}\right)^{\alpha}} \quad (1)$$

When analysing breakdown data, the characteristic parameter α for the Weibull distribution can be used as the breakdown voltage characteristic value, and characteristic β represents the dispersion size of the breakdown data. A Weibull probability paper is an important method for the Weibull distribution statistical test of experimental data [35].

III. EXPERIMENTAL RESULTS

A. BREAKDOWN VOLTAGE OF MO WITH NON-BRIDGING CELLULOSE PARTICLES UNDER LI STRESS

Figure 3 shows the Weibull cumulative breakdown probability plots for three concentrations of NB_CPS samples (i.e. 0.004 wt%, 0.008 wt% and 0.012 wt%) in MO against the CO sample for comparison. The LI breakdown voltage (LIBV) decreases with an increase in cellulose particle concentration.

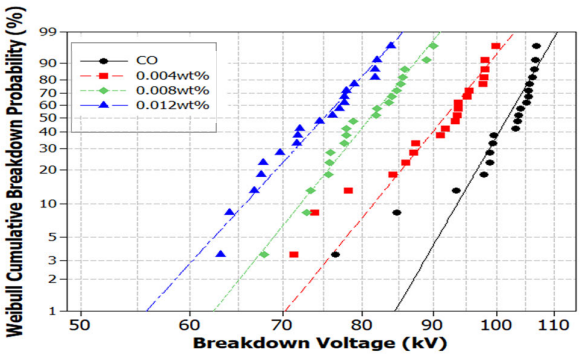

FIGURE 3. Weibull cumulative breakdown probability plots showing the effect of cellulose particle concentration (NB_CPS) on the LIBV of MO.

The results presented in Figure 3 and Table 1 show that the 50% breakdown voltage for the 0.004 wt%, 0.008 wt% and 0.012 wt% NB_CPS samples declined by 9.84%, 21.62% and 27.03%, respectively, compared with that of CO. This finding indicated that cellulose particle concentration may be responsible in enhancing the electrical field within the electrode gap, significantly influencing the reduction of the LIBV of MO. The results exhibit good agreement with those of Lu and Liu [25], [36], where cellulose particle concentrations were identified as dominant factors that influenced breakdown events in insulating oil.

TABLE 1. Weibull distribution fitting parameters and LIBV for NB_CPS samples with different concentrations of cellulose particles (0.004 wt%, 0.008 wt% and 0.012 wt%).

Parameter	CO	0.004%	0.008%	0.012%
Water Content (ppm)	6.08	7.67	7.63	7.86
50% Breakdown Voltage (kV)	102.01	91.97	79.96	74.43
Shape Parameter **(α)**	22.61	16.01	16.16	13.87
Scale Parameter **(β)**	103.55	93.80	81.78	76.59

B. BREAKDOWN VOLTAGE OF MO WITH BRIDGING CELLULOSE PARTICLES UNDER LI STRESS

Figure 4 shows the Weibull cumulative breakdown probability plots for different concentrations of B_CPS samples in MO. The Weibull fitting parameters and LIBV of B_CPS are listed in Table 2. The LIBV of the 0.004 wt%, 0.008 wt% and 0.012 wt% B_CPS samples declined by 23.71%, 23.73% and 26.91%, respectively, compared with that of the CO sample. The results exhibited no significant differences in LIBV amongst sample concentrations. However, LIBV was considerably different for 0.004 wt% and 0.008 wt% compared with that in NB_CPS, except for 0.012 wt%. The reduction in LIBV was relatively identical to that in NB_CPS at the same cellulose particle concentration. This finding indicated that the same breakdown mechanism may occur because of bridge formation within the gap.

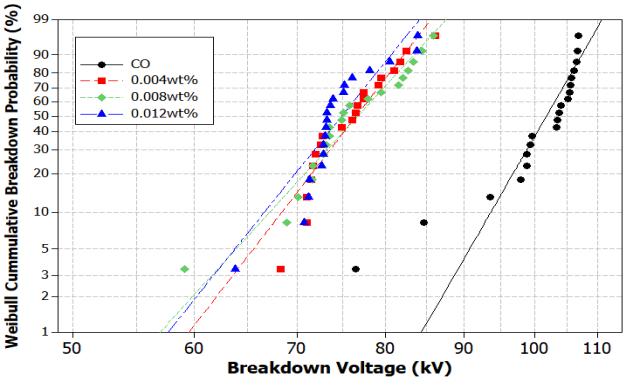

FIGURE 4. Weibull LIBV probability plots of various cellulose particle concentrations with bridging (B_CPS) in MO.

TABLE 2. Weibull distribution fitting parameters and LIBV FOR B _CPS samples with different concentrations of cellulose particles (0.004 wt%, 0.008 wt% and 0.012 wt%).

Parameter	CO	0.004%	0.008%	0.012%
Moisture Content (ppm)	6.08	7.67	7.63	7.86
50% Breakdown Voltage (kV)	102.01	77.82	77.80	74.55
Shape Parameter **(α)**	22.61	16.85	14.25	16.22
Scale Parameter **(β)**	103.35	78.24	78.74	76.62

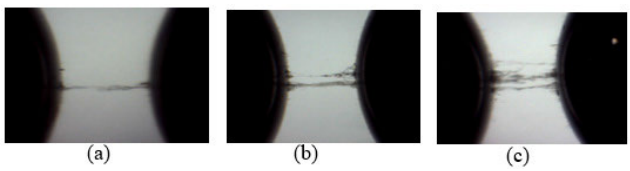

FIGURE 5. Bridge formation of B_CPS samples at different cellulose particle concentrations: (a) 0.004%, (b) 0.008% and (c) 0.012% with weight captured at the same time (40 s).

Figure 5 shows the microscopic optical images of the bridge formation of the B_CPS samples at different cellulose

particle concentrations. Although the density of the cellulose that bridges the gap slightly increased with cellulose concentration, LIBV remained relatively the same. The LIBV for 0.004 wt%, 0.008 wt% and 0.012 wt% B_CPS (Table 2) is 77.82, 77.80 and 74.55 kV, respectively. The LIBV for 0.012 wt% B_CPS is relatively identical to that for 0.012 wt% NB_CPS (Table 1). Nevertheless, the 0.004 wt% and 0.008 wt% cellulose particles exhibit varying LIBV between B_CPS and NB_CPS. This finding is discussed further in the next section.

As listed in Table 2, the LIBV values of B_CPS are practically identical amongst the three cellulose particle concentrations in B_CPS. Apparently, the bridge skeleton (B_CPS) in MO is the primary factor why LIBV is low but does not contribute to the instantaneous breakdown of oil. The LIBV of B_CPS occurs at 74.55, 77.80 and 77.82 kV for 0.012 wt%, 0.008 wt% and 0.004 wt%, respectively, after a rising step voltage was applied. With the exception of 0.012 wt% cellulose concentration, 0.004 wt% and 0.008 wt% depicted different LIBV values for B_CPS and NB_CPS. Further investigation was conducted to understand this breakdown mechanism.

IV. ELECTRIC FIELD DISTRIBUTION

This section simulates electric field strength, intensity and uniformity electric flux lines within the electrode configuration gap with the presence of a bridge skeleton as shown in Figures 6 and 9. Modelling all the physics concepts that underlie the breakdown phenomenon in insulating oil is intrinsically complex. Therefore, several parameters, such as space charge behaviour and electric polarization, were excluded from the simulation. In the current study, the electric potential between two spherical electrodes (each with a radius of 13 mm and separated by a gap distance of 2 mm) was predicted using a 2D, symmetrical and steady-state model. Under static condition, the relationship between the electric potential (φ) and electric field (E) is given by

$$E = -\nabla\varphi. \tag{2}$$

The charge conservation equation in accordance with Gauss's law is given by

$$\boldsymbol{\varepsilon_0}\nabla \boldsymbol{V} = \mathbf{0}, \tag{3}$$

where $\boldsymbol{\varepsilon_0}$ is the vacuum permittivity (8.854×10^{-12} F/m), and V is the applied voltage.

Impulse waveform is generated by applying the injected voltage on the basis of the experiment data via the equation of impulse.

$$\boldsymbol{V_{imp}} = \boldsymbol{V}\left[\boldsymbol{e}^{(-\alpha t_F)} - \boldsymbol{e}^{(-\beta t_T)}\right]; \tag{4}$$

$$\boldsymbol{\alpha} = \frac{\mathbf{1}}{\boldsymbol{R_T C_I}}, \quad \boldsymbol{\beta} = \frac{\mathbf{1}}{\boldsymbol{R_F C_L}}; \tag{5}$$

$$\boldsymbol{t_F} = \boldsymbol{R_F C_L}, \quad \boldsymbol{t_T} = \boldsymbol{R_T C_I}; \tag{6}$$

$$\boldsymbol{\eta} = \frac{\boldsymbol{V_{imp}}}{\boldsymbol{Vin.}}; \tag{7}$$

where V_{imp} is the impulse voltage, V is the peak voltage, α is the wave tail-dependent constant, β is the wave front-dependent constant, t_F is the front time and t_T is the tail time. C_I is the impulse capacitor, C_L is the load capacitor, R_T is the tail resistor, R_F is the front resistor, η is the efficiency factor of the system and V_{in} is the input voltage. The value of V_{imp} from the experiment was assigned as the input voltage in the finite element analysis (FEA).

Figure 6 presents the cellulose bridge formation images of the 0.012 wt% NB_CPS sample captured by a camera at 10%, 20%, 30%, 40% and 50% of 75 kV impulse breakdown voltage. The images in the figure show that the natural behaviour of cellulose accumulated on the electrode's surface is tending to tailgate others to form long cellulose structures at every non-breakdown impulse shot. The cellulose that accumulated and expanded onto a long cellulose structure was influenced by impulse shot percentages until a thin bridge formation at 50% impulse breakdown voltage was completed. Accordingly, bridge development was initiated from a single cellulose, and its length extension was controlled by an impulse shot. At an impulse voltage of 10%, the cellulose began to form a bridge with an initial length of 0.78 mm. Then, the cellulose extended to 0.87 mm when impulse voltage was shot at 20%. Bridge formation was prominent at 30%–50% of the impulse shot voltage. Table 3 provides the length of cellulose that bridged the gap at each impulse shot percentage.

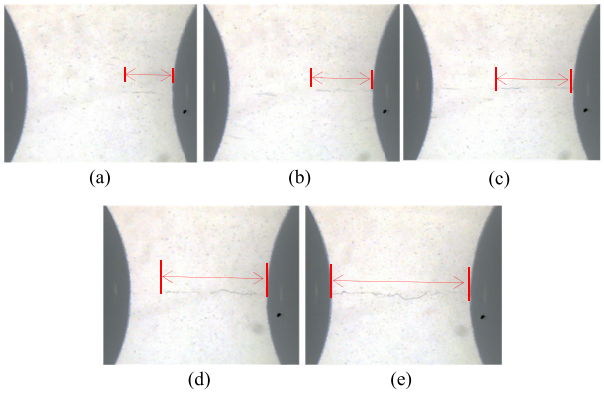

FIGURE 6. Microscopic pre-breakdown phenomenon images of single particles merging as a long cellulose formation at the designated non-breakdown of impulse shot at (a) 10%, (b) 20%, (c) 30%, (d) 40% and (e) 50% from the estimated critical field to breakdown (75 kV), indicating that cellulose tends to tailgate to form a long cellulose structure at each impulse shot, and subsequently, a thin naturally completed bridge.

TABLE 3. Influences of designated non-breakdown of impulse shot on natural cellulose formation during the NB_CPS experiment, where LIBV is 75 kV.

% of Impulse Shot	10	20	30	40	50
Length of Cellulose (mm)	0.8	0.9	1.2	1.5	2.0

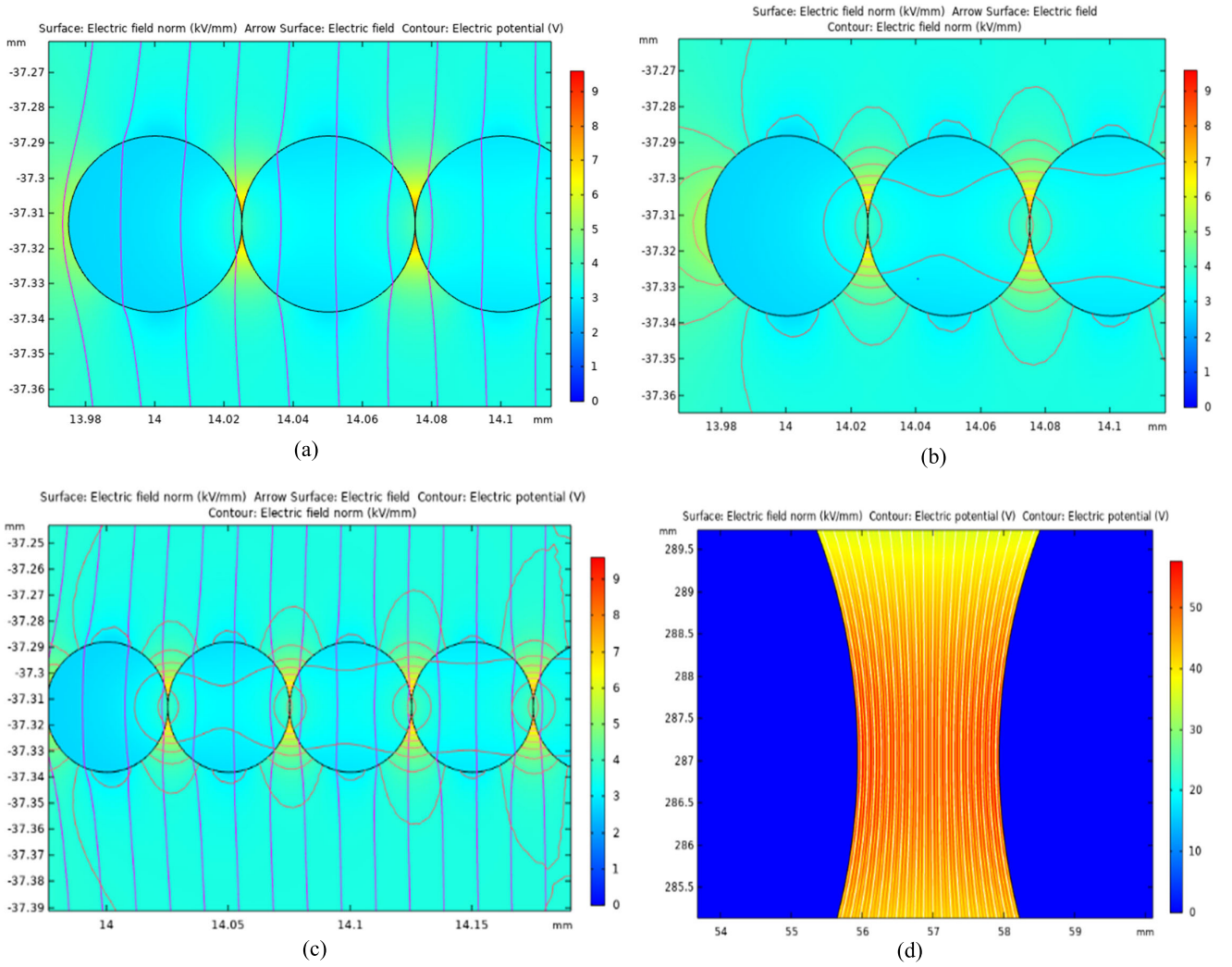

FIGURE 7. Simulation results of the electric field lines: (a) the presence of cellulose distorted the field lines, (b) field distortion continued on the cellulose surface, (c) field further distorted along the bridge skeleton and (d) ordinary quasi-uniform field lines when cellulose was absent (CO).

Cellulose bridge formation was extended at each designated impulse shot. Cellulose was polarised at each impulse shot and tended to extend by attracting other polarised cellulose particles and merging as a strong cellulose structure. The process was continued until a bridge skeleton formed between the gap. From the observation of images captured by a CCD camera, cellulose particles completely formed a bridge across the gap at 37.5 kV impulse voltage (50% of the impulse breakdown voltage) without breakdown. As the applied impulse voltage increased further and approached the breakdown voltage, more cellulose particles attached onto the existing cellulose bridge formation, resulting in a thick density of cellulose bridge network across the gap because of the cellulose particle concentration in oil. At 37.5 kV, i.e. 50% of the applied impulse voltage, the electric field distribution across the oil gap that contained 0.012 wt% of NB_CPS may not exceed the critical electric field of the insulating oil.

The permittivity of MO was 2.2, its conductivity was 5×10^{-9}s/m [37] and cellulose permittivity was 4.2 [28]. The cellulose radius was 0.5 mm, and the length of the cellulose skeleton was based on the result obtained from Figure 6. The cellulose clearly distorted the electric field lines whilst creating its own non-uniform flux line on the cellulose surface and its surrounding, as illustrated in Figures 7(a) and 7(b). The non-uniform flux lines were extended when another cellulose was suspended in oil, and the process was continued until a complete bridge was formed between the gap, as shown in Figure 7(c). The high field stress and intensity obtained between individual cellulose particles potentially led to a local breakdown near individual cellulose. Field distribution was distorted in swing patterns and continuously deteriorated as cellulose began to grow into a long cellulose skeleton, as shown in Figures 8(a), 8(b), 8(c), 8(d) and 8(e). The electric field strength of the bridge cellulose particles exceeded the critical electric field of CO only at 75 kV

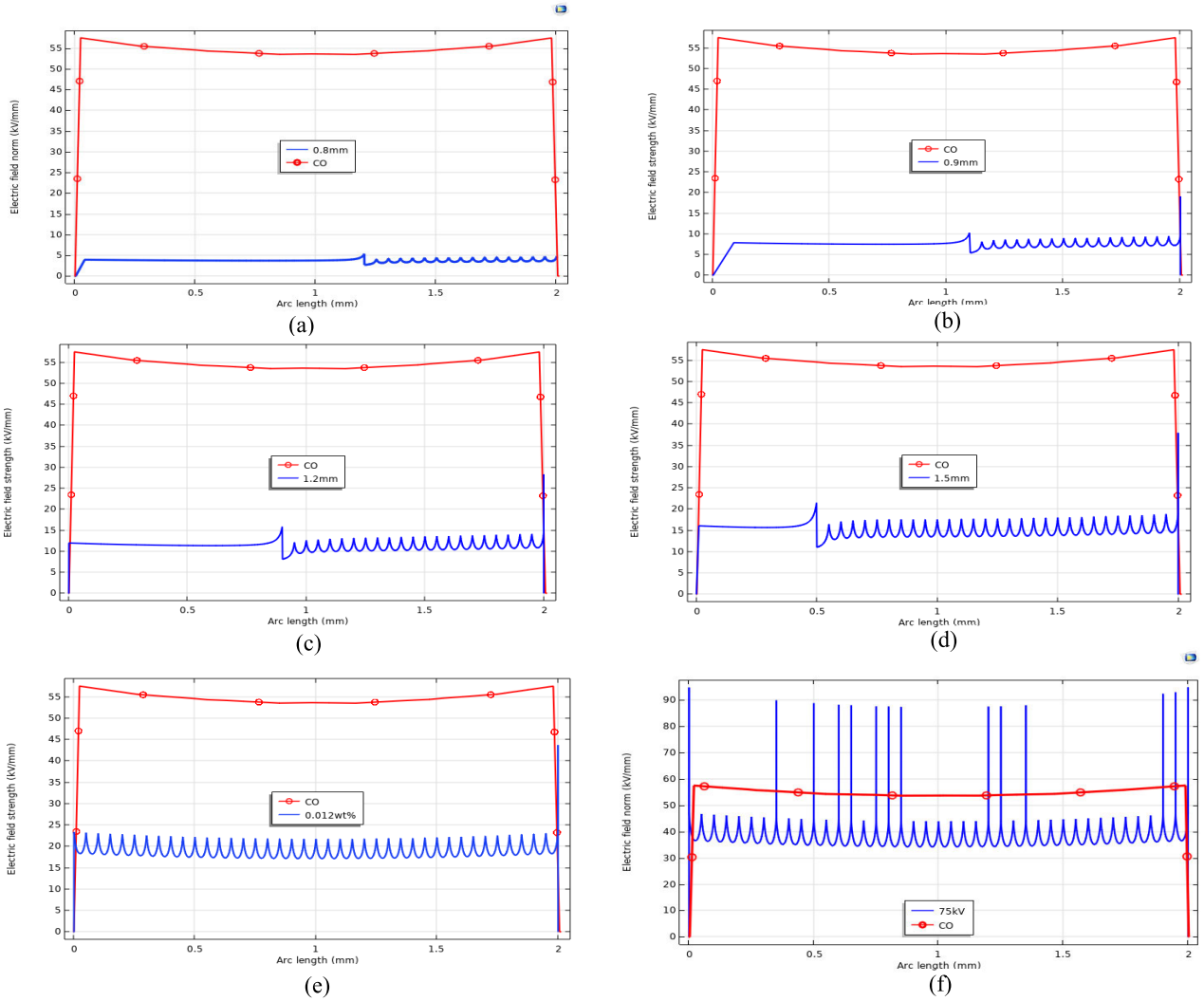

FIGURE 8. Swing patterns in the electrical field strength pre-breakdown phenomenon of cellulose merging as a long cellulose formation at the designated non-breakdown of the impulse shot at (a) 10%, (b) 20%, (c) 30%, (d) 40%, (e) 50%, and (f) 100% from LIBV (75 kV), indicating that cellulose influences the breakdown voltage of the liquid.

of the lightning impulse shot [Figure 8(f)] where LIBV occurred. In addition, the breakdown event was investigated further in the 0.004 wt% NB_CPS sample. Figure 9 shows the digital microscopic optical images of cellulose particles at 0.004 wt% when a bridge was still absent. The non-breakdown values of the impulse step voltage were applied from 60% to 90% of the breakdown voltage (92 kV). Cellulose movement remained unchanged when impulse voltage was shot from 10% to 60%. However, cellulose began to intensify, accumulate and attempt to form small pre-bridge cellulose particles as impulse voltage was applied from 70% to 80%. Accumulation progress was significant at 90%. The lengths of the pre-bridge cellulose particles for impulse voltages of 80% and 90% were 0.25 mm and 0.35 mm, respectively. However, a complete bridge skeleton could not be formed because the amount of polarised cellulose dispersed in oil was insufficient for attracting and merging others onto a long cellulose structure that can bridge the gaps, as shown in Figure 10(d).

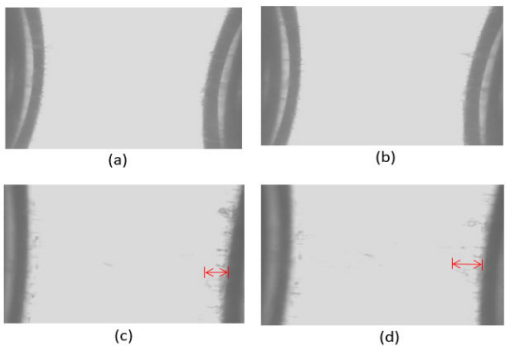

FIGURE 9. Microscopic optical images of cellulose accumulating to form a long cellulose structure at (a) 60% (b) 70%, (c) 80%, and (d) 90% of the non-breakdown impulse shot (92 kV) for 0.004 wt%, indicating that concentration influences cellulose merging to bridge gaps. The length of cellulose is 0.25 mm and 0.35 mm as observed in (c) and (d), respectively.

The evidence obtained in the current study indicated that a lower percentage of cellulose concentration in NB_CPS will not form a bridge across the gap, yielding to different

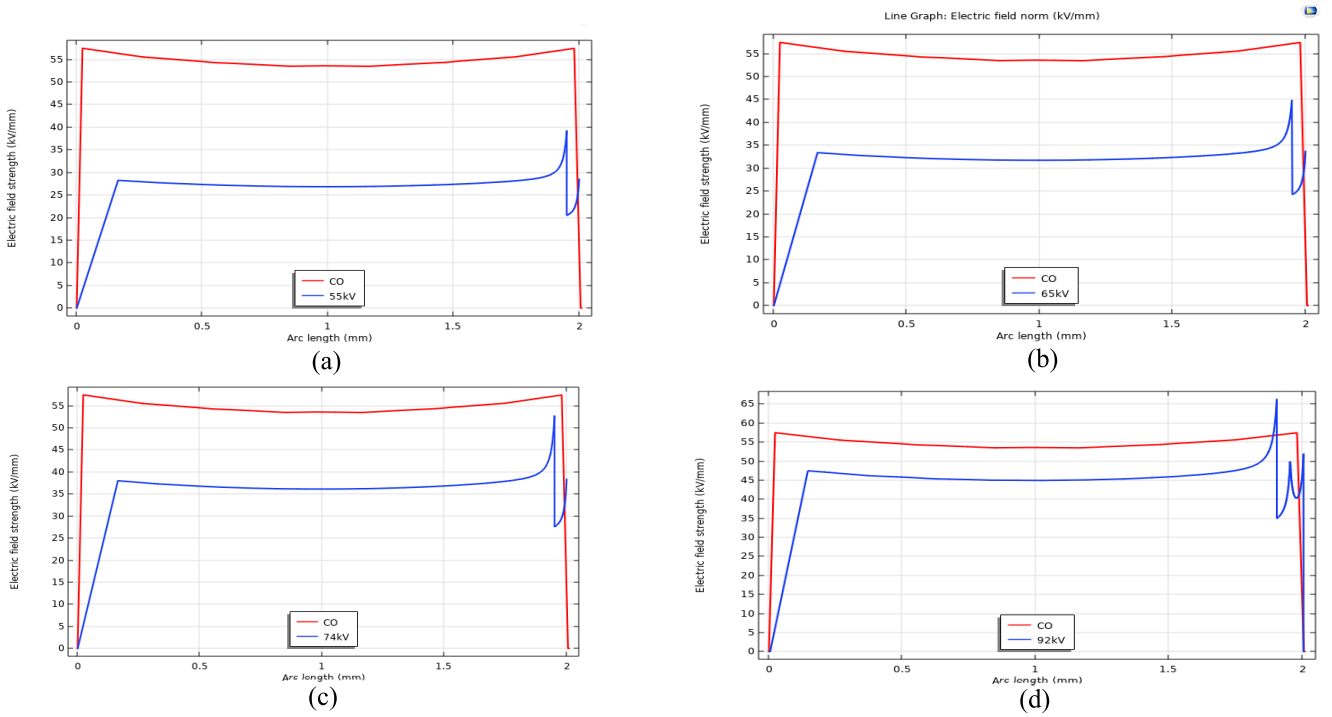

FIGURE 10. Electrical field strength and distribution of cellulosic accumulation at the designated non-breakdown of the impulse shot at (a) 70%, (b) 80%, (c) 90%, and (d) BDV from the estimated breakdown voltage (92 kV), indicating that the accumulation of cellulose length influences the breakdown strength of the liquid.

LIBV values for B_CPS with 0.004 wt%. The same trend was observed in 0.008 wt% NB_CPS.

Figure 10 depicts the electrical field strength along the line and across the cellulose accumulation with a length of 0.25 mm and 0.35 mm. The simulation was modelled from the results presented in Figure 9. The simulation of the electric field distribution shown in Figures 10(a), 10(b) and 10(c) was based on the impulse shot at 70%, 80% and 90% from the breakdown voltage of 92 kV with a pre-bridge cellulose particle length of 0.25 mm. Meanwhile, Figure 10(d) illustrates the electric field distribution at 0.35 mm cellulose length accumulation.

The result presented in this figure showed that electric field strength slightly increased to the level of impulse step voltage shot. At this point, however, no breakdown occurred because the field strength cannot break the critical electric field of the reference CO. Cellulose tended to accumulate to form a long cellulose structure within the vicinity of the electrode to bridge the gaps, as shown in Figure 9(d).

As depicted in Figure 10(d), the electrical field strength of 0.004 wt% was obtained at 66 kV/mm. This field strength exceeded the field strength of CO at 55 kV/mm, which was 20% above the critical withstand field of CO, and consequently, was committed and responsible for initiating the breakdown in the liquid

V. CONCLUSION

The influence of the cellulose particle contamination of MO with (B_CPS) and without (NB_CPS) bridge formation on LIBV was investigated. The LIBV of NB_CPS decreased gradually by 9.84%, 21.62% and 27.03% with an increase in cellulose concentration of 0.004 wt%, 0.008 wt% and 0.012 wt%, respectively. The detrimental effect was further enhanced when cellulose contamination was in the form of bridge skeleton. The LIBV of B_CPS decreased by 23.7% for 0.004 wt% and 0.008 wt% and further declined by 26.91% for 0.012 wt%. Under the same condition, the 50% breakdown voltage of MO was always comparable with that of CO.

At respective of non-breakdown of impulse shot, cellulose particles tended to accumulate and formed a thin bridge skeleton. Although cellulose particles formed a bridge across the gap, no instantaneous breakdown occurred because the local electric field was lower than the critical field of CO. This finding may provide knowledge and guidelines for the condition assessment and monitoring of contamination concentration to minimise common issues in power transformer failures that are attributed to the insulation system. The transformer is ensured to be fit for service and the integrity of the insulation system is optimum by monitoring the contamination level of the dielectric liquid.

Although most of the components in the transformer are in a quasi-uniform field, a non-uniform electric field may always be generated within the transformer. Broken copper windings or protrusions on the disk surface are potential causes that can lead to the initiation of discharges locally, contributing to local electric field enhancement and eventually resulting in the breakdown phenomenon. The results of further study will demonstrate the relationship between

bridge formation (along with bridge density) and the breakdown strength of MO in a non-uniform electric field. Bridge formation is expected to increase intensely due to strong dielectrophoresis forces, and the breakdown strength MO will decrease in the divergent field. Accordingly, no instantaneous breakdown will occur although cellulose particles bridge the gap.

REFERENCES

[1] A. M. Alshehawy, D. E. A. Mansour, M. Ghali, M. Lehtonen, and M. M. F. Darwish, "Photoluminescence spectroscopy measurements for effective condition assessment of transformer insulating oil," *Processes*, vol. 9, no. 5, pp. 1–15, 2021, doi: 10.3390/pr9050732.

[2] S. S. M. Ghoneim, K. Mahmoud, M. Lehtonen, and M. M. F. Darwish, "Enhancing diagnostic accuracy of transformer faults using teaching-learning-based optimization," *IEEE Access*, vol. 9, pp. 30817–30832, 2021, doi: 10.1109/ACCESS.2021.3060288.

[3] J. Hao, R. Liao, L. Yang, and Z. Ma, "Influence of natural ester on frequency dielectric response of impregnated insulation pressboard," *IET Sci. Meas. Technol.*, vol. 6, pp. 403–411, Jul. 2012, doi: 10.1049/iet-smt.2011.0180.

[4] L. E. Lundgaard, W. Hansen, D. Linhjell, and T. J. Painter, "Aging of oil-impregnated paper in power transformers," *IEEE Trans. Power Del.*, vol. 19, no. 1, pp. 230–239, Jan. 2004, doi: 10.1109/TPWRD.2003.820175.

[5] *Effect of Particles on Transformer Dielectric Strength*, Work. Study Committe, Cigre, Paris, France, Jun. 2000, vol. 12.

[6] S. Mahmud, G. Chen, I. O. Golosnoy, G. Wilson, and P. Jarman, "Experimental studies of influence of DC and AC electric fields on bridging in contaminated transformer oil," *IEEE Trans. Dielectr. Electr. Insul.*, vol. 22, no. 1, pp. 152–160, Feb. 2015, doi: 10.1109/TDEI.2015.004846.

[7] D. Wang, M. Sigurdson, and C. D. Meinhart, "Experimental analysis of particle and fluid motion in AC electrokinetics," *Exp. Fluids*, vol. 38, pp. 1–10, 2005, doi: 10.1007/s00348-004-0864-5.

[8] S. Birlasekaran, "The movement of a conducting particle in transformer oil in AC fields," *IEEE Trans. Electr. Insul.*, vol. 28, no. 1, pp. 9–17, Feb. 1993.

[9] C. L. Wadhwa, "Breakdown mechanism of gaseous, liquid and solid materials," in *High Voltage Engineering*, 3rd ed. New Delhi, India: New Age Science, 2012, pp. 18–23.

[10] J. Zhang, J. Li, D. Huang, X. Zhang, S. Liang, and X. Li, "Influence of non-metallic particles on the breakdown strength of vegetable insulating oil," in *Proc. Annu. Rep. Conf. Electr. Insul. Dielectr. Phenomena (CEIDP)*, no. 1, Dec. 2015, pp. 609–612, doi: 10.1109/CEIDP.2015.7352123.

[11] X. Wang and Z. D. Wang, "Particle effect on breakdown voltage of mineral and ester based transformer oils," in *Proc. Annu. Rep. Conf. Electr. Insul. Dielectric Phenomena*, Oct. 2008, pp. 598–602, doi: 10.1109/CEIDP.2008.4772859.

[12] C. L. Wadhwa, "Breakdown mechanism of gaseous liquid and solid materials," in *High Voltage Engineering*. New Delhi, India: New Age International, 2012, pp. 1–55.

[13] M. Wang, A. J. Vandermaar, and K. D. Srivastava, "Review of condition assessment of power transformers in service," *IEEE Elect. Insul. Mag.*, vol. 18, no. 6, pp. 12–25, Nov. 2002, doi: 10.1109/MEI.2002.1161455.

[14] S. Mahmud, G. Chen, I. O. Golosnoy, G. Wilson, and P. Jarman, "Bridging in contaminated transformer oil under AC, DC and DC biased AC electric field," in *Proc. Annu. Rep. Conf. Electr. Insul. Dielectric Phenomena*, Oct. 2013, vol. 472, no. 1, Art. no. 012007, doi: 10.1088/1742-6596/472/1/012007.

[15] J. S. N'cho, I. Fofana, A. Beroual, T. Aka-Ngnui, and J. Sabau, "Aged oils reclamation: Facts and arguments based on laboratory studies," *IEEE Trans. Dielectr. Electr. Insul.*, vol. 19, no. 5, pp. 1583–1592, Oct. 2012, doi: 10.1109/TDEI.2012.6311504.

[16] J. K. Nelson and C. Shaw, "The impulse design of transformer oil-cellulose structures," *IEEE Trans. Dielectr. Electr. Insul.*, vol. 13, no. 3, pp. 477–482, Jun. 2006, doi: 10.1109/TDEI.2006.1657958.

[17] International Electrotechnical Commission, *Power Transformers Part 3: Insulation Levels, Dielectric Tests and External Clearances in Air*, document IEC 60076-3, 2001.

[18] V. V. Sokolov and A. Lokhanin, "Internal insulation failure mechanisms of HV equipment under service conditions," in *Proc. CIGRE Conf.*, 2002, pp. 1–6.

[19] V. V. Sokolov, "Failure statistics. Transformer and bushing design review. Typical failures modes and failure causes. What can are learned from post mortem inspection," in *Proc. 5th AVO New Zeal. Int. Tech. Conf.*, 2006, pp. 1–14. [Online]. Available: http://www.lordconsulting.com/images/stories/TechnicalPapers/pdf/2006-Conference_VSokolov1.pdf

[20] H. Miyao, K. Endo, M. Higaki, Y. Kamato, and Y. Kato, "Influence of micro particles in fluid on the impulse and AC breakdown strengths of low-viscosity silicone liquid immersed insulating systems," in *Proc. IEEE Int. Electr. Eng.*, Okinawa, Japan, Oct. 2008, p. 146.

[21] W. Ziomek, "Transformer electrical insulation," *IEEE Trans. Dielectr. Elect. Insul.*, vol. 19, no. 6, pp. 1841–1842, Dec. 2012.

[22] S. S. M. Ghoneim, S. S. Dessouky, A. Boubakeur, A. A. Elfaraskoury, A. B. A. Sharaf, K. Mahmoud, M. Lehtonen, and M. M. F. Darwish, "Accurate inuslating oil breakdown voltage model with different barrier effects," *Processes*, vol. 9, no. 657, p. 16, 2021. [Online]. Available: https://www.mdpi.com/journal/processes

[23] J. Xiang, Q. Liu, and Z. D. Wang, "Streamer characteristic and breakdown in a mineral oil and a synthetic ester liquid under DC voltage," *IEEE Trans. Dielectr. Electr. Insul.*, vol. 25, no. 5, pp. 1636–1643, Oct. 2018, doi: 10.1109/TDEI.2018.006938.

[24] O. Lesaint, "'Streamers' in liquids: Relation with practical high voltage insulation and testing of liquids," in *Proc. IEEE Int. Conf. Dielectr. Liq. (ICDL)*, Jul. 2008, pp. 1–6, doi: 10.1109/ICDL.2008.4622543.

[25] W. Lu and Q. Liu, "Effect of cellulose particles on impulse breakdown in ester transformer liquids in uniform electric fields," *IEEE Trans. Dielectr. Electr. Insul.*, vol. 22, no. 5, pp. 2554–2564, Oct. 2015, doi: 10.1109/TDEI.2015.005097.

[26] *Nytro Gemini X- High Grade Mineral Oil*. Nynas AB, Stockholm, Sweden, 2012. [Online]. Available: http://www.nynas.com/Segment/Transformer-oils/Our-transformer-oil-products/Nytro-Gemini-X—High-grade

[27] International Electrotechnical Commision, *IEC 60897-Methods for the Determination of the Lightning Impulse Breakdown Voltage of Insulating Liquids*, document CEI/IEC 60897, 1987.

[28] C. K. Lieu, "Safety data sheet," in *SIGMA-ALDRICH (M) SDN BHD Level 3*, M. S. Annexe, J. L. Timur, and B. Sunway, Eds. Selangor, Malaysia. St. Louis, MI, USA: Sigma-Aldrich, 2021. [Online]. Available: http://www.sigmaaldrich.com

[29] S. Mahmud, G. Chen, I. O. Golosnoy, G. Wilson, and P. Jarman, "Bridging phenomenon in contaminated transformer oil," in *Proc. IEEE Int. Conf. Condition Monitor. Diagnosis*, Sep. 2012, pp. 180–183, doi: 10.1109/CMD.2012.6416405.

[30] S. Mahmud, G. Chen, I. O. Golosnoy, G. Wilson, and P. Jarman, "Bridging in contaminated transformer oil under AC, DC and DC biased AC electric field," in *Proc. Annu. Rep. Conf. Electr. Insul. Dielectric Phenomena*, Oct. 2013, pp. 943–946, doi: 10.1109/CEIDP.2013.6747424.

[31] E. Kuffel, S. W. Zaengl, and J. Kuffel, "High voltage measuring and techniques," in *High Voltage Engineering*, J. K. E. Kuffel, Ed. Oxford, U.K.: Newnes Butterworth-Heinemann, 2001, pp. 490–491.

[32] Y. V. Torshin, "Prediction of the impulse breakdown voltage of the mineral transformer oil from predischarge phenomena," All-Russian Electrotechnical Inst. (VEI), Moscow, Russia, Tech. Rep. D1-101, CIGRE 2012, 2012.

[33] P. N. Mikropoulos, C. A. Stassinopoulos, and B. C. Sarigiannidou, "Positive streamer propagation and breakdown in air: The influence of humidity," *IEEE Trans. Dielectr. Electr. Insul.*, vol. 15, no. 2, pp. 416–424, Apr. 2008, doi: 10.1109/TDEI.2008.4483460.

[34] J. Li, Z. He, and S. Grzybowski, "Electrical aging lifetime model of oil-impregnated paper under pulsating DC voltage influenced by temperature," *IEEE Trans. Dielectr. Electr. Insul.*, vol. 20, no. 6, pp. 1992–1997, Dec. 2013.

[35] J. Li, Y. Wang, and L. Bao, "Two factors failure model of oil-paper insulation aging under electrical and thermal multistress," *J. Electr. Eng. Technol.*, vol. 9, no. 3, pp. 957–963, May 2014.

[36] W. Lu and Q. Liu, "Effect of cellulose particles on streamer initiation and propagation in dielectric liquids," in *Proc. IEEE 11th Int. Conf. Properties Appl. Dielectric Mater. (ICPADM)*, Jul. 2015, pp. 939–942, doi: 10.1109/ICPADM.2015.7295428.

[37] T. Judendorfer, A. Pirker, and M. Muhr, "Conductivity measurements of electrical insulating oils," in *Proc. IEEE Int. Conf. Dielectric Liquids*, Jun. 2011, pp. 4–7, doi: 10.1109/ICDL.2011.6015456.

SARIZAN BIN SAAIDON was born in Perak, Malaysia, in 1979. He received the bachelor's degree (Hons.) in electrical engineering from the University Technology of MARA (UiTM), in 2003. He is currently pursuing the Ph.D. degree with Universiti Sains Malaysia. He worked as a Technical Executive at PSC Naval Dockyard after receiving his bachelor's degree. He joined the Advanced Technology Centre (ADTEC) Kulim and the Industrial Technical Institute, in 2003, and the Head of the Division when he transferred to the Industrial Training Institute at Kepala Batas, since 2006. He is also a Certified Instructor of ILSAS for underground cable system up to 33 kV and transformer maintenance systems. He is currently the Head of Coordination for CIAST Satellite Campus in Kepala Batas, Pulau Pinang. He is also a member of BEM and a Professional Technologist (MBOT). Aside from conducting research in HV liquid area, he is also interested and appointed in a panel of judges in Junior Skill Malaysia Competition (Electrical Technology Installation). He was also a Gold Medal Holder for major innovation competition, such as i-INNOVA, MTE, ITEX, CiTEC, and i-COMPEX, and Robotic Competition/Robocon (Best Design Award-South East Asia Robot Competition 2012).

MOHD AIZAM TALIB received the bachelor's degree in electrical engineering from the University of Portsmouth, U.K., in 1997, and the Ph.D. degree in electrical engineering from Universiti Teknologi Malaysia, in 2016. Upon his graduation in 1997, he worked with ABB Transmission and Distribution Sdn Bhd as a Design Engineer. Since 1998, he has been employed at TNB Research Sdn Bhd as a Research Engineer. He currently holds the position of a Technical Expert (Transformer Diagnostic). His research interests include transformer condition monitoring, and insulation diagnostic and dielectric measurements.

MOHAMAD NUR KHAIRUL HAFIZI ROHANI received the Diploma degree in computer engineering, the B.Eng. degree (Hons.) in industrial electronic engineering, and the Ph.D. degree in electrical system engineering from the University Malaysia Perlis, Malaysia, in 2010, 2013, and 2017, respectively. He currently works as a Senior Lecturer and the Program Chairperson of Diploma of electrical engineering at the Faculty of Electrical Engineering Technology, Universiti Malaysia Perlis. He is also a Research Fellow with the High Voltage Centre of Excellence for Renewable Energy (CERE) and a member of the High Voltage and Transient Insulation Health Research Group. His research interests include partial discharge detection and measurement on solid and liquid insulation, signal and image processing, and partial discharge sensor development for high-voltage equipment applications.

NOR ASIAH MUHAMAD (Member, IEEE) received the bachelor's degree in electrical and electronic engineering from Universiti Teknologi PETRONAS, Malaysia, in 2002, the master's degree in electrical power engineering from the University of South Australia, in 2006, and the Ph.D. degree from the University of New South Wales, Australia, in 2009. She was a Researcher and a Senior Lecturer with the Faculty of Electrical Engineering, Institute of High Voltage and High Current (IVAT), Universiti Teknologi Malaysia. She is currently serving as a Senior Assistant Professor for Universiti Teknologi Brunei. She also acts as an Associate Professor with the School of Electrical and Electronic Engineering, Universiti Sains Malaysia. Her research interests include power system equipment monitoring, in particular insulation diagnosis and the development of new systems for condition monitoring. Beside doing research in HV area, she also works in energy efficiency and integration for domestic and industrial area in Malaysia.

MOHAMAD KAMAROL MOHD JAMIL (Senior Member, IEEE) received the B.Eng. degree (Hons.) in electrical engineering from Universiti Teknologi Mara, Malaysia, in 2000, and the M.Eng. and D.Eng. degrees from the Kyushu Institute of Technology, Japan, in 2005 and 2008, respectively. In 2002, he joined Universiti Sains Malaysia (USM) with a University ASTS Fellowship. He was later a Senior Lecturer, in 2008, and was promoted to an Associate Professor, in 2014. He was a Senior Engineer at Sankyo Seiki (M) Sdn. Bhd. for almost eight years. He was a Visiting Researcher with the High Voltage Laboratory, Kyushu Institute of Technology, from 2013 to 2014, and the Chiba Institute of Technology, Japan, in February 2020. His research interests include the insulation properties in oil palm, solid dielectric material, insulation properties of environmentally benign gas, and PD detection technique for insulation diagnosis of power apparatus and electrical machine. He is also involved in temperature rise and short-circuit electromagnetic study of busbar systems and HVDC systems. He is a Professional Engineer and a Chartered Engineer, and a member of the IET, the Board of Engineers Malaysia, and the Institution of Engineers Malaysia. Within the doctor course study, he received the Chatterton Young Investigator Award from the IEEE International Symposia on Discharges and Electrical Insulation in Vacuum, in 2006.